

Economic power dispatch solutions incorporating stochastic wind power generators by moth flow optimizer

Mohammad Khurshed Alam^{1*}, Mohd Herwan Sulaiman¹, Md. Shaoran Sayem² and Rahat Khan³

Faculty of Electrical & Electronics Engineering Technology, Universiti Malaysia Pahang (UMP), 26600 Pekan, Pahang, Malaysia¹

Faculty of Electrical & Electronics Engineering Technology, American International University-Bangladesh, Dhaka²

Faculty of Electrical Engineering, Minnesota State University 228, Wiecking Center, Mankato, MN 56001, United States³

Received: 13-September-2022; Revised: 20-February-2023; Accepted: 22-February-2023

©2023 Mohammad Khurshed Alam et al. This is an open access article distributed under the Creative Commons Attribution (CC BY) License, which permits unrestricted use, distribution, and reproduction in any medium, provided the original work is properly cited.

Abstract

Optimization encourages the economical and efficient operation of the electrical system. Most power system problems are nonlinear and nonconvex, and they frequently ask for the optimization of two or more diametrically opposed objectives. The numerical optimization revolution led to the introduction of numerous evolutionary algorithms (EAs). Most of these methods sidestep the problems of early convergence by searching the universe for the ideal. Because the field of EA is evolving, it may be necessary to reevaluate the usage of new algorithms to solve optimization problems involving power systems. The introduction of renewable energy sources into the smart grid of the present enables the emergence of novel optimization problems with an abundance of new variables. This study's primary purpose is to apply state-of-the-art variations of the differential evolution (DE) algorithm for single-objective optimization and selected evolutionary algorithms for multi-objective optimization issues in power systems. In this investigation, we employ the recently created metaheuristic algorithm known as the moth flow optimizer (MFO), which allows us to answer all five of the optimal power flow (OPF) difficulty objective functions: (1) reducing the cost of power generation (including stochastic solar and thermal power generation), (2) diminished power, (3) voltage variation, (4) emissions, and (5) reducing both the cost of power generating and emissions. Compared to the lowest figures provided by comparable approaches, MFO's cost of power production for IEEE-30 and IEEE-57 bus architectures is \$888.7248 per hour and \$31121.85 per hour, respectively. This results in hourly cost savings between 1.23% and 1.92%. According to the facts, MFO is superior to the other algorithms and might be utilized to address the OPF problem.

Keywords

Multi-objective economic-environmental power dispatch (MOEED), Probability density functions (PDFs), Combined cost and emission minimization, Success history-based adaptation technique of differential evolution (SHADE).

1. Introduction

Numerous generating units, load locations, and tens of thousands of buses contribute to the vastness and integration of today's electrical networks. Many different solutions have been put up to deal with issues relating to optimal power flow (OPF). In a typical power flow, the values of the control variables are given. A set goal can only be enhanced (minimized or maximized) in the event that all or some of the control variables in an OPF are understood.

The OPF computation has numerous applications, including power systems, real-time control, operational planning, and problems [1].

OPF is used by a lot of modern energy management systems (EMS). With increasing power system scale and interconnection complexity, OPF is becoming more important [2] in a neural network. The OPF should, for instance, help with deregulation transactions or make suggestions regarding the type of reinforcement that is required. An improvement in the utilization of an existing asset (such as generating or transmitting) or the provision of a less expensive substitute for the construction of new facilities is

* Author for correspondence

referred to as a control option. It minimizes an objective function constrained by equality and inequality through a first-order gradient approach. Solution approaches were despised because they required more computer resources than typical power flow processes. The next generation OPF has been upgraded since power system management or planning needs to know the limit, the cost of electricity, the incentive for adding units, and the construction of transmission networks for a specific load entity. The demand for an OPF tool to evaluate the situation and recommend corrective actions for both offline and online research has grown since the first OPF study was published in the 1960s. The need for OPF to manage challenges in the current deregulated industry as well as unresolved concerns in the vertically integrated business has made it more difficult to evaluate the potential and talents of the existing OPF. In 1981, Happ [3] released the first comprehensive study on optimal power dispatch, and Fioretto et al. [4] quickly followed. A bibliographical analysis of the most important economic-security functions and absolute loss approximations [5] was published in 2018. There are two types of problem-solving strategies: traditional (classical) approaches and innovative solutions. OPF has often been successfully fought utilizing standard techniques. In recent years, a detailed investigation has been conducted into the use of these technologies. Conventional techniques based on the ideas of mathematical programming can be used to handle OPF problems of various sizes. To be able to fulfill the demands of several goal functions, application kinds, and limitations, traditional classical methods are further categorized into the following categories: Methodologies such as the customized sequential quadratic programming [6], the gradient method [7], genetic algorithm method [8–11] and particle swarm optimization (PSO) [12–14], are some examples of the available methods. In recent years, new strategies that are backed by artificial intelligence (AI) have been made with the goal of fixing problems with analytical techniques. Artificial neural networks (ANN) [15], ant colony algorithm [16–19], fuzzy logic [20], multiobjective optimization [21, 22], a flexible alternating current transmission system (FACTS) [23], quadratic programming [24], interior point optimization [25, 26], and locational electricity [27] are some of the methods discussed. The fact that intelligent procedures may frequently adjust to a wide array of qualitative restrictions is the primary benefit offered by these methods. These methods allow for the presentation of several potentially optimal options within a single simulation. OPF is becoming

increasingly important as the number and sophistication of power system interconnections continue to increase. Since time immemorial, people have held the opinion that determining the optimal flow of power while using traditional (thermal) generators possesses non-linear limitations and is a difficult non-linear issue. The fact that breeze and cosmic energy exist in the sporadic origin of power makes the situation more difficult. This article explains how to maximize power flow in a system that combines traditional thermal power with the variable breeze and cosmic as examples of energy sources. The Weibull and lognormal probability density function (PDF) are utilized in the process of energy forecasting for wind and solar energy subsequently.

In the target consequence, both the conserved price of overestimating intermittent renewable sources and the penalty cost of underestimating those sources are taken into account. The emission component is also addressed in the objectives of the case study [28]. Wind turbines (WT) and solar (also known as photovoltaic (PV) energy provide the greatest challenge when it comes to integrating them as a result of the unpredictable environment of their achievement. The majority of wind, including solar-producing plants, are privately owned and operated by their own companies. Power purchase agreements (PPAs) are negotiated between the grid/ independent system operator (ISO) and the companies in question (scheduled power). However, on rare occasions, in light of the variable output of numerous sustainable power sources, the energy production may exceed expectations, leading to an underestimate of the capacity that is actually available. This can occur when there is a surplus of renewable energy sources. If more electricity is not utilized, the fee will be covered by ISO. An overestimation occurs when the power that is generated is lower than the power that was forecasted. When adopting ISO, you will need a spinning reserve in order to cut down on the amount of power that is consumed, which will make the system's maintenance expenses higher. The OPF objective function that is given below takes into account all of the associated expenses, including those associated with the production of thermal power units as well as the costs of using sustainable energy directly, penalty, and in reserves. The Weibull PDF is utilized to simulate the distribution of wind speed, whereas the lognormal PDF is utilized to simulate the distribution of solar irradiance. This study revises the IEEE-30 bus and IEEE-57 bus systems so that they may manage renewable energy

sources like wind and solar electricity. The cost of production is brought down, and an investigation into the most efficient scheduling is carried out in connection to alterations in reserve and penalty costs. Thermal generators fueled by fossil fuels do not produce harmful gases into the atmosphere, in contrast to sustainable energy. Carbon taxes resembling levied in several countries and are recalculated according to the number of conservatory emissions produced. In the case studies that were selected to explore the effect of the influence on generator scheduling, the amount of the carbon price was tied to the target function. In this article, the grey wolf optimization (GWO) [29] method of optimizing case studies is discussed. The use of fuzzy selection allowed for an investigation of the potential effects of the OPF issue for valve-point loading and generator emission [30]. OPF control for a hybrid PV, gasoline power, and battery-separated technique is depicted in [31, 32]. It was suggested in [33, 34] that a comparable free-standing hybrid system that includes PV cells, WT, and diesel generators might consider using pumped hydro storage as an option for energy storage. Adding renewable sources of power like solar and wind to the grid is the subject of a number of articles that have been published. However, the primary emphasis of these papers was placed on the effectiveness of the generators, as well as the various pricing strategies implemented by the ISO as well as the utility operator. The minute-to-minute variance of renewable energy sources was the subject of research that was carried out so that economic efficiency might be improved. A diesel generator and an optimization platform were the components that made up the hybrid system that was described in [35]. The shortcomings of traditional methodology are intended to be addressed by moth flow optimizer (MFO) techniques. Qualitative restrictions can be accommodated using MFO algorithms. MFO approaches provide good outcomes for multipurpose constraint situations. In many instances, they can find the optimal answer on a global scale.

Detailed objectives include the following:

- a) The invention of an indigenous MFO design to address the OPF issue.
- b) MFOs for stochastic wind energy are incorporated into well-known standard bus interfaces such as IEEE 30 and IEEE 57.
- c) A statistical analysis of the OPF solution, as well as a comparison of MFO to previous versions of metaheuristic algorithms.
- d) In this study, five distinct single-objective OPF solutions utilizing MFO are examined: cost, loss,

voltage variation, emission, cost-effectiveness, and carbon footprint reduction.

The main purpose of this research is to find ways to provide continuous and cost-effective power. The rest of the paper is structured as follows: Section 2 is a literature review of how the OPF was set up, and section 3 is about the methods used to solve the OPF. In section 4, the results of the investigation are summarized. Section 5 discussed the constraints, and section 6 discussed the conclusion and future work.

2.Literature review

To solve the optimization issue, success history-based adaptive differential evolution (SHADE) was applied [36]. The probability of finding a suitable location drops as the population of the area drops, and the algorithm might not find any feasible solutions at all, or it might find answers that aren't quite as good as the ones it was looking for. Because of this, linear success history-based adaptive differential evolution (L-SHADE) is the primary explore design utilized if a constraint handling (CH) approach is required to resolve restrictions. Because of this, it is guaranteed that the determination of the worldwide optimum of a limited, multimodal system, nonlinear optimization challenge will be accurate and prompt. In order to meet operational requirements and load demand while also lowering operating fuel costs and pollution levels, combined economic and emission dispatch (CEED) challenges are being developed by MFO [37–39]. Using the moth's modified path in a new spiral around the flame, an updated version of the dramatist's MFO design called the superiority of feasible solution moth flow optimization (SF-MFO) was introduced. Additionally, the suggested SF-MFO has been used to solve the CEED issue, and its performance is compared with those of other optimization techniques. For attaining the best economic power dispatch solutions, the barnacles mating optimizer [40] numerical method was studied. The technique of large-scale PV [41], IoT-based intelligent fault detection and normalization of a power distribution system [42], Bangladesh's future energy needs and potential for wind power [43], performance analysis of non-renewable energy in Bangladesh [44], affordable clean energy transition in developing countries [45] make use of control parameters and gains from attributes of the MFO process. The size of the optimization is reduced via optimal reactive power dispatch (ORPD), radial distribution network (RDN), control parameters, shunt capacitor (SC), hybrid active power filter (HAPE) compared to

discretization in the time domain, issue. Thus, the resulting method doesn't worry about system nonlinearities, is quick to implement, and has a lower computing complexity. It has been used and evaluated on two real-world issues. Results indicate that in ideal circumstances, the approach could generate stabilizing controls. It is advised to test it out on SF-MFO structures for future development. All of these studies looked at situations involving a single target for optimization. Within the context of the multi-objective economic environmental power dispatch (MOEED), the current research focuses on power distribution made possible by using relatively small-scale generators of hydroelectric, solar, wind, and thermal power. In this paper, a review of several optimization techniques utilized to solve OPF problems was conducted. The OPF technologies are fundamentally split between traditional methods and

artificial intelligence (AI) methods. Different sizes of OPF problems, which are mathematically grounded, are solved using conventional approaches. The rebuilt network is made up of thermal, breeze, and cosmic PV generators. Energy generation from wind in *Figure 1* and solar PV in *Figure 2* is flexible. *Figure 1* displays the breeze velocity frequency distributions including weibull fitting following 8000 Monte-Carlo runs with parameters set to 9 and 2. *Figure 3* indicates the valve-loading effect for dual power generator. The consequent modifications of MFO implementation are shown in *Figure 4*. All producing outputs and reserves must be combined to adjust power output variances. All running expenses for the generator including dual fire generators, fines, and reserve charges are included in the total production costs. Examples of various parameter settings are displayed in *Tables 1* and *2*.

Table 1 provides an overview relating to the IEEE-30 bus system under discussion

Elements	Amount	Feature
Feeders	30	[40]
Subdivide	41	[40]
Thermoelectric Turbines (TG1,TG2,TG3)	3	Feeders:1(swing),2 and 8
Wind Turbines (WG1,WG2)	2	Feeders:5 and 11
PV Solar units(SPV)	1	Feeder:13
Constant tolerant	11	Scheduled real power for five generators, including SPV, TG1, TG2, TG3, WG1 and WG2, as well as voltages on the bus for every generator bus (6 Nos.)
Load Connected	-	283.4 MW, 126.2 MVar
Voltage span in load Feeder	24	[0.96–1.06] p.u

Table 2 PDF characteristics pulse wind energy bus coefficients at 11

Nominal capacity	Dissemination	Shortest price amount (\$/WM)	Amount of conserve price (\$/MW)	Amount of fine price (\$/MW)
40 MW	$M=6, \sigma=0.6$	$g_{sG}=1.6$	$K_{ps}=3$	$K_{ps}=1.5$

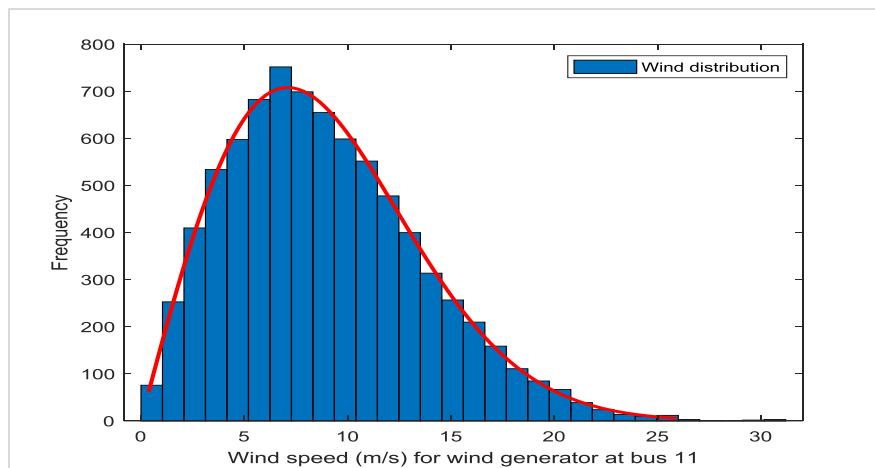


Figure 1 Wind generator at bus 11

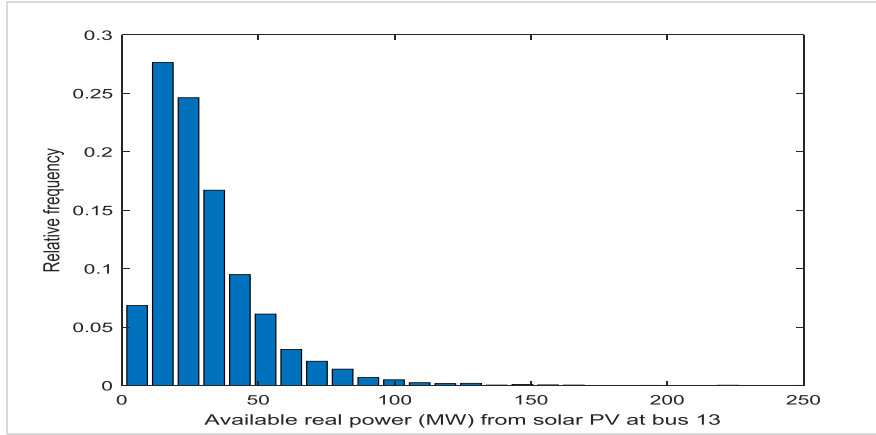


Figure 2 PV solar at bus 13

A few recent articles [39, 43] have discussed the integration of renewable energy sources such as wind and solar into the grid. Despite this, the great majority of these efforts focused on the utility operator's and ISO's respective real-time scheduling of generators for cost-effective operation. We investigated the minute-to-minute variability of renewable energy sources with the goal of optimizing dispatch. The hybrid system was composed of stochastic solar power using the barnacle's mating optimizer and the MATLAB optimization platform stated in [40] for the OPF solution. Although network restrictions are sometimes disregarded in the economic dispatch (ED) problem, they must be met in OPF. Furthermore, the ED problem is frequently confused with the OPF problem, rather than the network voltage profile and emission properties. More research is needed to investigate OPF in a network that includes thermal, wind, and PV generators.

3. Methods

3.1 Thermal units

Fossil fuels are used to run thermal power plants. The equilateral [8] connection roughly reflects the connection between gasoline expenditure (\$/h) and energy output (MW) as shown in Equation 1:

$$F_{cost}(P_{TTG}) = \sum_{i=1}^{N_{TG}} \{a_i + b_i P_{TGi} + c_i P_{TGi}^2 + \{d_i \sin[e_i (P_{TGi}^{min} - P_{TGi})]\} \} \quad (1)$$

The cost coefficients of each generator are a_i , b_i , c_i , d_i , and e_i , and P_{TT} is all available power generated by heat-producing devices. P_{TGi} , where i is the i -th generator's lowest power setting, P_{TGi} is the overall count of thermal system generators, and N_{TG} a valve loading impact.

3.2 Reducing the cost of renewable energy production

When incorporating renewable energy sources into the electrical grid, several issues must be taken into consideration, including their erratic and sporadic nature. In general, solar PV and wind farms are controlled by private businesses that engage in a PPA with an ISO. As a result, the prices incurred by such power sources are broken down into three groups: direct costs, reserve costs, and finally punishment costs. Here are the straight costs of generators that are powered by wind and solar PV [34], which are also considered in Equations 2 and 3:

$$Cost_{wj}(P_{wGj}) = g_{wGj} P_{wGj} \quad (2)$$

$$Cost_{s,k}(P_{sGk}) = g_{sGk} P_{sGk} \quad (3)$$

Where g_{wGi} and g_{sGk} depart direct cost factors for the j th and k th wind power plants, respectively. In equation 4, P_{wG} , J , and P_{sG} , K show how much electricity is expected to come from wind and solar power plants.

$$Cost_{SHG}(P_{SHG}) = Cost_{(PSG+PHG)} = g_{SG} P_{SG} + g_{HG} P_{HG} \quad (4)$$

The direct cost coefficients for solar PV, g_{SG} , and g_{HG} are PHG , g_{Sg} , and g_{HG} , respectively. It should be highlighted that the agreed-upon ISO-agreed-upon anticipated power production is set, and that this energy will be delivered feeder through cosmic PV and mini cogeneration combined units. The element is frequently operated at full capacity due to micro hydro's limited capacity and volatility because cogeneration power output varies with river flow rate, assuming a run-of-river configuration, a continuous head.

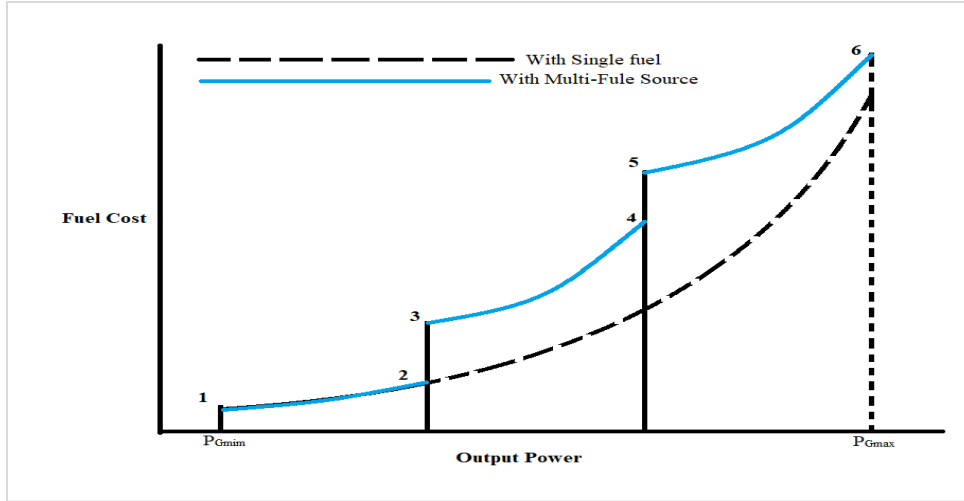


Figure 3 Price curve for only one and dual fire generator[46]

The actual quantity of energy produced by the sun and wind farms are likely to be reduced than predicted. Figure 4 depicts the MFO implementation, and Figure 5 depicts the modified IEEE 30. This is characterized as power overestimation from an unknown source, and the system operator must plan define and classify occasions to guarantee continuous service to almost clients. The price of allocating reserve-producing modules [34] is inflated, even for wind and solar power generation, as shown in Equations 5 and 6.

$$Cost_{RWj}(P_{WGj} - P_{Way,j}) = K_{RWj}(P_{WG,j} - P_{Way,j}) = K_{RW,j} \int_0^{P_{WG,j}} (P_{WG,j} - P_{W,j}) f_w(P_{W,j}) d_{pW,j} \quad (5)$$

$$Cost_{RSK}(P_{SG,k} - P_{Sav,k}) = K_{RS,k} \times f_s(P_{Sav,k} < P_{SG,K}) \times [P_{Sav,k} < P_{SG,K} - E(P_{Sav,k} < P_{SG,K})] \quad (6)$$

Where $P_{Wav,j}$ stands actual for capacity available through the j th a wind turbine (WT) $K_{RW,j}$ is the reserve price factor for that plant, and $f_w(P_{W,j})$ denotes wind energy likelihood densification formula of that plant. The definite energy output through the k th cosmic PV station is $P_{Sav,k}$ the conserve price factor for that plant is $K_{RS,k}$, the expectation that cosmic PV power will be less dissimilarity. $P_{SG,k}$ is $f_s(P_{Sav,k})$, and the expectation that solar PV power will be less than $P_{SG,K}$ is $E(P_{Sav,k} < P_{SG,k} (P_{Sav,k}))$. In equation 7, the following example shows how the cost of the reserve for a combination of solar PV and small-scale hydropower is inflated:

$$Cost_{RSH}(P_{SHG} - P_{SHav}) = K_{RSH}(P_{SHG} \times P_{SHav}) = K_{RSH} \times f_{SH}(P_{SHav} < P_{SHG}) \times [P_{SHG} - E(P_{SHav} < P_{SHG})] \quad (7)$$

Where $f_{SH}(P_{SHav} P_{SHG})$ what likelihood there is combined solar and small hydropower shortage relative to P_{SHG} and $E(P_{SHav} P_{SHG})$ is anticipated that tiny hydropower and solar electricity will fall beneath P_{SHG} , K_{RSH} the cost elasticity of the integrated system, P_{SHav} the real energy produced by the same factory, and $P_{SHav} P_{SHG}$ is the likelihood of this occurring. When power is overestimated, real delivered power may be more than expected values, producing surplus power. Each problem must be solved by putting a cost fine on the problem that is proportional to the amount of extra energy. This may be shown in Equation 8 to the order of solar and breeze-producing facilities, respectively:

$$Cost_{PWj}(P_{Wav,j} - P_{WGj}) = K_{PW,j} \int_{P_{WG,j}}^{P_{Wtr,j}} (P_{W,j} - P_{WG,j}) f_w(P_{W,j}) d_{pW,j} Cost_{PS,K}(P_{Sav,k} - P_{SG,k}) = K_{PS,K}(P_{Sav,k} - P_{SG,K}) \quad (8)$$

In which $P_{wr,j}$ is a rated output same source of the power wind farm, $K_{PW,j}$ the cost of penalties for the j th wind power project, $K_{PS,K}$ is the cost-of-penalty factor for the k th PV solar array, and $f_s(P_{Sav,k} > P_{SG,K})$ indicate the likelihood that renewable solar PV energy will be more than expected. The expectation for solar PV is given by P_{SHG} and $E(P_{SHav} P_{SHG})$.

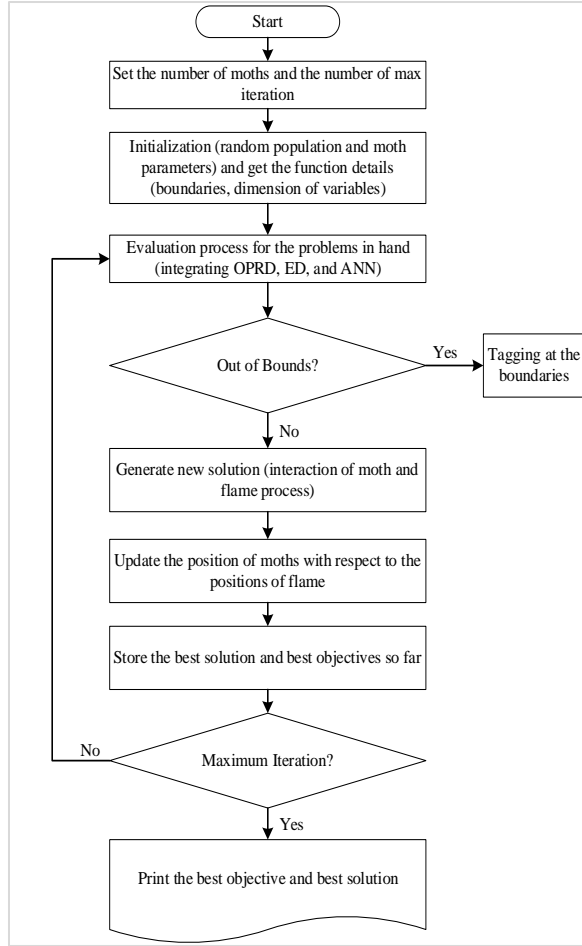


Figure 4 MFO implementation

3.3 Loss reduction

The second intention of OPF is shown in Equation 9 as reducing total actual transmission system power outages, which is defined as the sum of all energy waste [32] in the transmission network:

$$F_{Loss} = \sum_{nl} \sum_{j \neq i}^{nl} G_{ij} [V_i^2 + V_j^2 - 2V_i V_j \cos(\delta_i - \delta_j)] \quad (9)$$

In which V_i and V_j represent along transmitting and the recipient voltages as regards buses i & j , G_{ij} transmitting conductance lines i - j , and nl is how many transmissions lines in the energy system.

3.4 Decrease in voltage fluctuation

Even though Equation 10 shows that the ultimate target of OPF is to get rid of voltage changes on all buses in the electrical system's network, this is not how it works in practice:

$$F_{VD} = \sum_{m=1}^{nL} |V_{LM} - 1.0| \quad (10)$$

Where nL indicate quantity of energy feeders and V_{Lm} , which is voltage on the load feeder.

3.5 Generation of electricity and emission reductions

This objective function solely applies to thermal power generation, which emits greenhouse gases SO_x , NO_x , and CO_2 out into the air. The Equation 11 shows some ways to reduce emissions [37]:

$$F_{Emission} = \sum_{i=1}^{nTG} [a_i + \beta_i P_{TGi} + \gamma P_{TGi}^2 + \omega_i e^{(u_i P_{TGi})}] \quad (11)$$

In this case α_i , β_i , γ_i , ω_i and μ_i represent the exhalation factor for the i -th generator, including the valve loading impact lowering the power generation and pollution. Putting in place a carbon price to decrease emissions of greenhouse gases is the third objective that needs to be investigated.

$$F_{CE} = F_{cost} + c_i F_{Emission}$$

Where c_i represents the \$20 per hour carbon tax [27].

3.6 Constraints

All potential OPF solutions must fulfill all equality and inequality standards. To meet the equality criteria, the real and reactive power Equations 12 and 13 must be satisfied, as shown below [3]:

$$P_{Gi} - P_{Di} - V_i \sum_{j=1}^{nB} V_j [G_{ij} \sin(\delta_{ij}) + B_{ij} \cos(\delta_{ij})] = 0 \forall i \in nB \quad (12)$$

$$Q_{Gi} - Q_{Di} - V_i \sum_{j=1}^{nB} V_j [G_{ij} \cos(\delta_{ij}) - B_{ij} \sin(\delta_{ij})] = 0 \forall i \in nB \quad (13)$$

P_{Gi} and Q_{Gi} reflect active plus combative energy output at the bus i (together with breeze and cosmic power), P_{Di} and Q_{Di} represent actual and combative power at the feeder i , and nB represents the system's total number of buses. Where ij is the voltage angle that sets apart bus j from bus i . In contrast, the functioning restraint of the energy structure components are inequality constraint, which can be shown by Equations 14 through 20:

$$P_{TGi}^{min} \leq P_{TGi} \leq P_{TGi}^{max} \quad i=1, N_{TG} \quad (14)$$

$$P_{WG}^{min}, j \leq P_{WG,j} \leq P_{WG,j}^{max}, j = 1, \dots, N_{WG} \quad (15)$$

$$P_{SG,k}^{min} \leq P_{SG,k} \leq P_{SG,k}^{max} \quad k=1, N_{SG} \quad (16)$$

$$Q_{TGi}^{min} \leq Q_{TGi} \leq Q_{TGi}^{max} \quad i=1, N_{TG} \quad (17)$$

$$Q_{WG,j}^{min} \leq Q_{WG,j} \leq Q_{SQ,k}^{max} \quad k-1, N_{SG} \quad (18)$$

$$Q_{SG,j}^{min} \leq Q_{SG,j} \leq Q_{TG,k}^{max} \quad k - 1, N_{SG} \quad (19)$$

$$V_{Gi}^{min} \leq V_{Gi} \leq V_{Gi}^{max}, i = 1, NG \quad (20)$$

Using the cost curve, this study explores the limited zones of thermal generators. To produce consistent results, entire thing limitations fall under the managed flow of energy software (MATPOWER).

3.7 Optimizer algorithms for different test cases

Three metaheuristic algorithms were investigated for use in addressing the OPF issue in this article. GWO, MFO, and SHADE are their names. They are discussed in the sections that follow.

3.7.1MFO FOR OPF

Origin moths have about 160,000 unique species, and their life cycles are like those of butterflies (i.e., a moth has two phases of life: larva and adult, where it is turned into a moth by whale). The unusual night navigation method of moths is the most interesting feature of their lives [47]. They have developed to fly at night with the help of moonlight. A transverse orientation navigation system was also used. It's a highly efficient means of traveling for long distances in a straight line, and this mechanism allows the moth to do so by keeping it at a consistent angle to the moon while it flies. Because the moon is so far away, this mechanism ensures that the moth remains on track. Humans may utilize a similar navigation approach. Assume the moon is on the south side of the sky and you want to go east. He will be able to walk straight toward the east if he walks with the moon on his left side. The moths do not fly forward but rather spiral around lights. This is because the transverse orientation strategy is only successful when the light source is very far away (moonlight). When moths are exposed to artificial light, they want to keep flying at the same angle. As a result, moths form spirals around lights.

3.7.2GWO for OPF

To reflect the wolf pack's own internal hierarchy, we classify the wolves as either alpha, beta, delta, or omega, with the top, second, and third rankings members being designated as alpha, beta, and delta, sequentially, and leftover members being classified as omega. See *Figure 5* for an explanation of how alpha, beta, and delta regulate the GWO's search behavior. They lead their pack members (W) to fruitful hunting grounds. Three wolves, designated as alpha, beta, and delta, evaluate the likely location of process prey during the iterative search process.

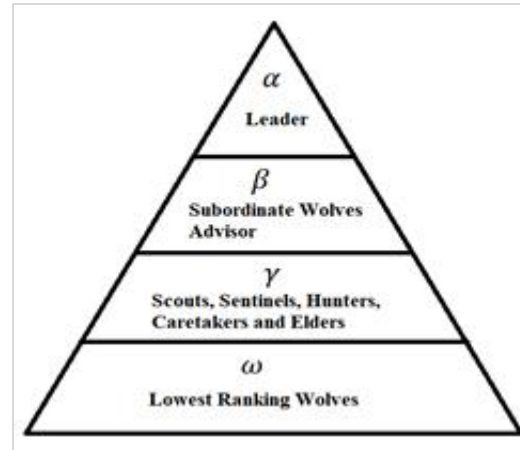


Figure 5 GWO considering OPF [29]

3.7.3SHADE for OPF

Differential evolution, which adjusts parameters based on past performance, is used to solve the optimization challenge. SHADE is an expert form of DE that takes into account past values of control parameters to inform decisions about what those parameters should be in the future. This ensures that the global optimums of a nonlinear optimization problem with constraints on several variables can be found rapidly and with high accuracy. SHADE is utilized in conjunction with the method for managing constraints that emphasizes the SF. Nearly all OPF literature uses a penalty function technique to identify restriction violations. The choice of the punishment coefficient has an impact on this method. Small penalty coefficients overuse the impractical region, extending the search for workable alternatives.

4. Results

4.1A system using IEEE 30 bus with the modifications listed below

The system is a customized version of the IEEE 30-bus scenarios, OPF simulations, and MATLAB for five different instances. In addition, the P_{TG2} no-fly zones are listed in *Table 2*. The pl value has been set to 21, the MFO population to 30, and the maximum iteration to 200. This section examines OPF-prediction accuracy and compares it to the SF model and one-dimensional approximation of the alternating current (AC) model. In addition, it evaluates numerous design decisions in depth. Data sets experiments investigate potential models from MATLAB, a variety of power networks (MFO, GWO, and SHADE). The analysis focuses mostly on the IEEE 30 and IEEE 57-feeder structure for ease of presentation. The results, however, are consistent across the full benchmark set. The ground truth data

are compiled in the following manner: Various benchmarks are developed for each network by varying the nominal load inside a variance of 20% consequently, the loads are sampled from the distributions. Consequently, the resulting benchmarks have load requirements that vary by up to 20% of their nominal values: Many of them become substantially more computationally difficult and crowded than their initial counterparts. The network value constituting the dataset entry possible and practicable for OPF explanation by addressing the SHADE issue. The MFO approach outperforms the SHADE algorithm, as expected. It should be observed that there are only a few iterations (mean of 4 outer iterations per run); nevertheless, MFO

algorithm is roughly 6 times slower than the SHADE algorithm, as expected, since the price (processing time) of a single SHADE solution is almost 1.5 times higher than that of a trust region.

Case 1: Lower manufacturing expenses

The objective here is to lower the expense of producing power using cogeneration power sources like those described in section 2. All breeze, celestial, cosmic PV, with a few hydro models make use of PDF features. MFO beat other comparison algorithms in all statistical analyses from 30 simulation runs, as shown in Table 3. MFO had the lowest cost of generation, 888.7248 \$/h, while GWO had the highest, 889.9486 \$/h.

Table 3 Statical results used in generation cost for different algorithms

Innovation	Minimum(MW)	Maximum(MW)	Average value(MW)	Standard deviation(MW)
SHADE	891.2346	892.6542	891.0876	1.234987
MFO	888.7248	891.1283	889.3877	0.998364
GWO	889.9486	894.0422	890.3444	2.522093

SHADE is utilized in conjunction with the method for managing constraints that emphasizes the SF. Nearly all OPF literature uses a penalty function technique to identify restriction violations. The choice of the punishment coefficient has an impact on this method. Small penalty coefficients overuse the impractical region, extending the search for workable alternatives. All algorithms produced the same operating points and succeeded in generating the solution in Figure 6.

\$10,720.488 would be accumulated (24 hours each day, 365 days per year, $24 \times 365 = 8760$ hrs \times \$1.2238=\$10,720.488).

Table 4 displays all the top outcomes for state variables and control variables from all methods. Table 5 demonstrates that the desired outcomes of the control variables and state variables for each approach fall within the predetermined limitations.

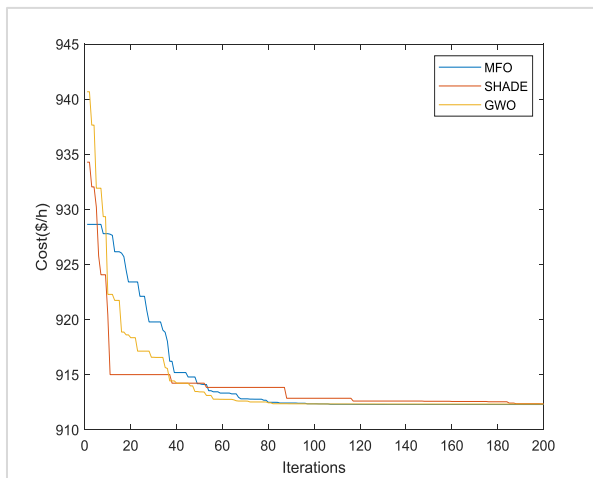


Figure 6 Convergence curve for generation cost

It's noteworthy that MFO and GWO arrive at vastly different results at \$1.2238 per hour. At a rate of \$1.2238 per hour for 8760 hours of saving, a total of 348

Apart from the SF, which generates 65 MW, all algorithms on thermal generator bus 2 avoided banned operation zones. In the appendix's Tables A1 and A2, the control variables for the IEEE-30 and IEEE-57 buses are displayed, respectively. This table also shows how long it takes to compute each algorithm. It should be noted that MFO ultimately performed better than other tactics even though it took more time to analyse the data. Parallel computing also could significantly lighten the computational load. The conclusion drawn from Table 3 and the previous scenarios is that it's ideal for the reversal cost to be as minimal as feasible, as in the first three hypotheses, in which the rated power of a wind farm is equal to the scheduled power of the wind farm, thereby minimizing thermal unit sharing and maximizing wind farm sharing, thereby lowering total generation cost. The deviation of load from two breeze units that was optimally scheduled in respect to reserve cost variations is shown in Figure. 1. The abbreviations and recommended method for

resolving OPF issues are presented in *Appendix I* and *Table A3*. The optimal projected load for the two breeze units lowers as load increases since less spinning reserve is required as expected. As seen in *Figure 3*, thermal generators raise outputs to make up

for energy farms' decreased outputs, which raises the cost of generation. As the penalty cost increases, *Figure 6* shows that the overall cost of generating remains relatively constant for two wind farms operating at their rated power.

Table 4 Optimal control variable findings for Cases 1-2

Item	Limit		Case 1		Case 2	
	Min	Max	GWO	MFO	GWO	MFO
Pg2	0.00	100.00	49.89	26.24	51.90	9.56
Pg5	0.00	140.00	75.00	75.00	136.69	140.00
Pg8	0.00	100.00	34.60	35.00	97.15	100.00
Pg11	0.00	550.00	57.44	60.00	315.76	315.96
Pg13	0.00	200.00	18.29	39.24	198.28	200.00
Vg1	0.00	210.00	1.06	1.06	210.00	210.00
Vg2	0.95	1.10	1.05	1.05	1.03	1.02
Vg5	0.95	1.10	1.04	1.04	1.07	1.10
Vg8	0.95	1.10	1.10	1.10	1.02	1.02
Vg11	0.95	1.10	1.10	1.10	1.04	1.02
Vg12	0.95	1.10	1.04	1.03	1.03	1.03
Vg13	0.95	1.10	1.03	1.02	0.98	1.10
Vg14	0.95	1.10	1.4	1.05	0.98	0.98
Cost(\$/h)			2.0108334562	1.73864886	31364.7846739117	29574.61785
Floss(MW)			2.106456965	2.07457453	20.05246417	19.68200787

Table 5 Results for case 1-2's state variables

State variables	Limit		Case1		Limit		Case 2	
	Min	Max	MFO	GWO	Min	Max	MFO	GWO
Pg1	50	200	50.86651	50.53166	0	450	376.01682	377.28608
			MW	MW			MW	MW
Qg1(Mvar)	-20	150.0	-20.00000	-20.00000	-140	200	28.61165	76.82446
Qg2(Mvar)	-20	60.0	21.49194	18.25091	-17	50	50.00000	50.00000
Qg5(Mvar)	-30	35.0	19.80614	21.87291	-10	60	47.61349	-1.89348
Qg8(Mvar)	-15	40.0	40.00000	40.00000	-8	25	12.86673	25.00000
Qg11(Mvar)	-25	30.0	30.00000	29.40358	-140	200	52.52669	57.82163
Qg13(Mvar)	-20	25.0	18.29288	21.26882	-3	9	9.00000	9.00000

4.1.2 Case 2: lowering transmission loss overall

The desired function in this instance is to lower total transmission loss. After running the load flow program, the MATPOWER then returns the total loss. The statistical outcomes of MFO are compared to those of several metaheuristic techniques in *Table 6*. This table shows that MFO, SHADE, and GWO are in order of decreasing loss. In terms of consistency, MFO outperforms SHADE, as

evidenced by highest, mean, and predictable error values by 30 simulation trial. *Figure 7* depicts a boxplot for all algorithms in this scenario, with the MFO and GWO attaining the lowest loss. *Table 6* highlights the full optimum findings achieved.

For control variables and state variables utilizing all methodologies. Both MFO and GWO provide closed findings with the same loss of 7.022743 MW.

Table 6 Minimization of total transmission loss

Innovation	Minimum(MW)	Maximum(MW)	Average value(MW)	Standard deviation(MW)
SHADE	7.033887	8.001233	7.091237	0.065432
MFO	7.022743	7.188386	7.064235	0.064396
GWO	7.995548	8.103882	7.246823	0.039223

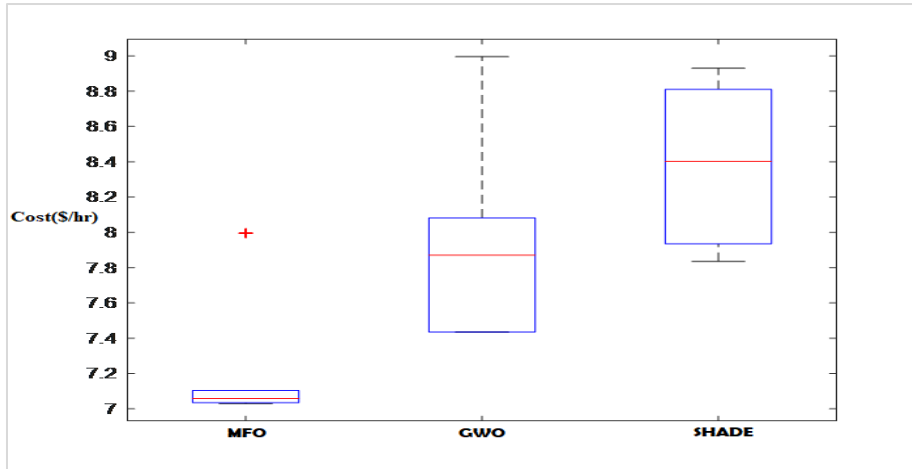


Figure 7 Transmission loss boxplot for all algorithms

The MFO is more accurate and efficient than the SHADE, as evidenced by a comparison of the price of used and energy losses between the two approaches. According to the data, the MFO is highly effective at resolving the OPF issue by lowering

distribution dropping and production prices rather than preserving network safety (potential standard lowest and highest load restriction). *Figure 8* depicts the voltage profile for the best algorithm run in this scenario; the range is within acceptable bounds.

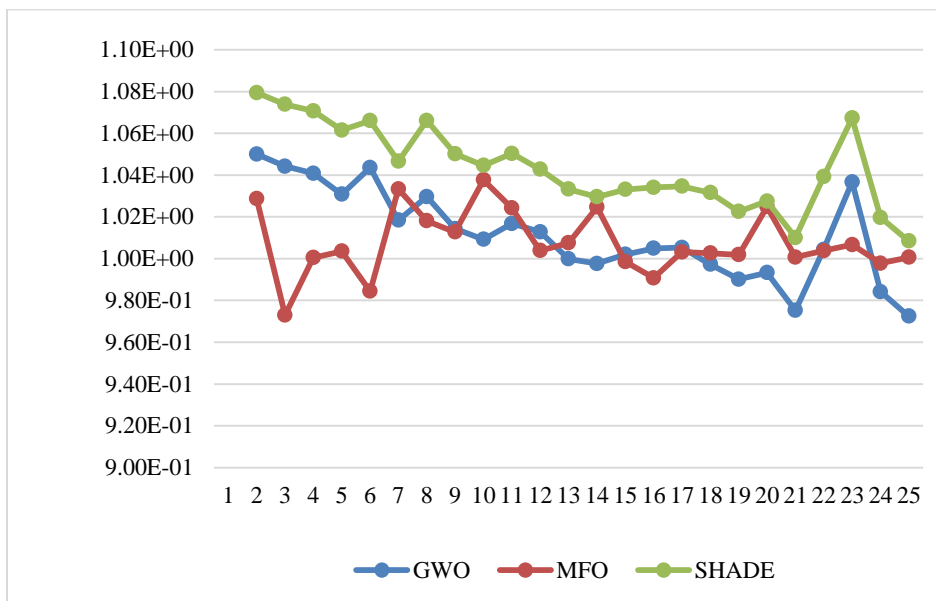


Figure 8 Voltage profile for IEEE 30 bus

4.1.3 Case 3: Voltage deviation has been reduced

For Case 3, reducing voltage difference is crucial since it represents the voltage quality every bus in a network of the electrical system. *Table 7* displays the simulation results for this situation.

MFO has been demonstrated to offer the greatest results in terms of lowest voltage fluctuation while

excelling in terms of maximum, average, and SD for lowest voltage fluctuation. *Figure 9* depicts the voltage profiles obtained by each approach at the load buses. Most of them seem very similar, with magnitudes between 0.98 and 1.05 p.u., with GWO being the most efficient in minimizing voltage volatility (0.0962 p.u.).

Table 7 Minimization of voltage deviation

Algorithms	Min(p.u)	Max(p.u)	Mean(p.u)	Std Dev(p.u)
SHADE	0.916542	1.062775	1.046523	0.062541
MFO	0.898822	1.05105527	1.03101	0.077822
GWO	0.953718	1.082556	1.038136	0.057878

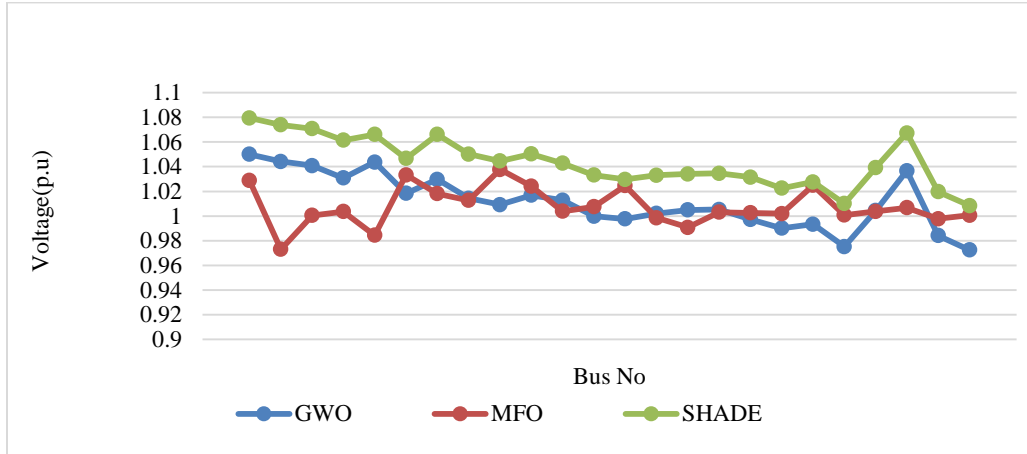


Figure 9 Characteristics of voltage for every algorithm

4.1.4 Case 4: emission reduction

In this instance, reducing emissions is the target function. The statistical findings from 30 simulations run for all methodologies are presented in *Table 8*. The performance of MFO in reducing emissions is

superior to that of any other method in designation of the lowest, highest, mean, and predictable error. The boxplot in *Figure 10* shows that MFO outperforms others in terms of all statistical descriptors.

Table 8 shows the emissions of different algorithms

Innovation	Minimum(\$/h)	Maximum\$/h)	Average value(\$/h)	Standard deviation(\$/h)
SHADE	1.3729425	1.410963	1.410752	0.003527
MFO	1.2405803	1.409189	1.408086	0.001542
GWO	1.392753	1.471462	1.420413	0.031498

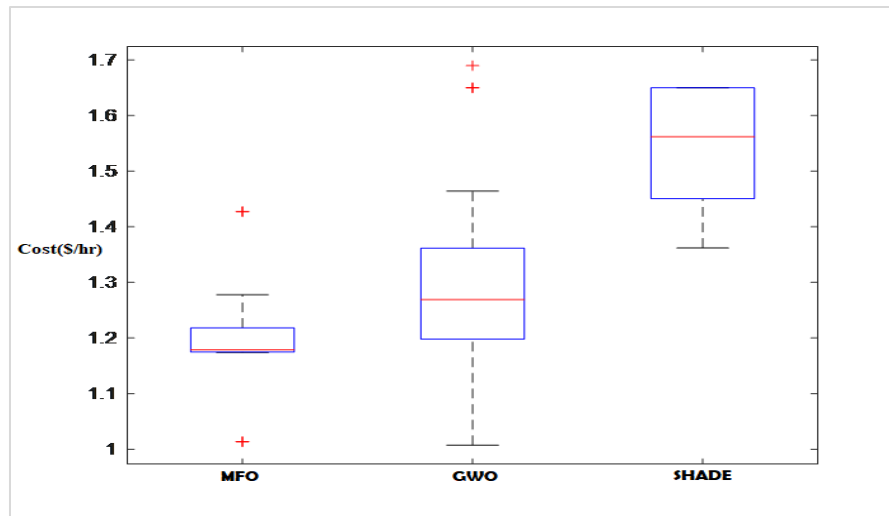


Figure 10 Boxplot for emission

4.1.5 Case 5: Cost reduction in generation and emissions

In this situation, the aim function to be reduced is the production cost, which includes the emission effect. Table 9 shows the statistical results of each method after 30 simulated attempts. MFO once more outperformed the other algorithms in terms of the lowest, medium, and highest costs of producing output from 30 simulation trials.

The lowest cost per unit of production is held by MFO (47.16332 \$ per hour), followed by GWO

(48.6827 \$ per hour). The cost difference between MFO and GWO is \$1.51938/h, which equates to a cost reduction year of $\$1.51938/h \times 8760 \text{ h} = \13309.7688 . Utilizing renewable energy sources like wind, solar, and hydropower is encouraged by carbon pricing. After 30 runs of algorithms, Figure 11 depicts the distribution findings obtained by all boxplots for this situation. This graph clearly shows that MFO surpasses other algorithms in terms of accuracy.

Table 9 Reduction of production and emissions costs

Innovation	Minimum(\$/h)	Maximum(\$/h)	Average value(\$/h)	Standard deviation(\$/h)
SHADE	49.64231	52.90654	49.6579	0.924567
MFO	47.16332	51.32719	49.7018	0.921646
GWO	48.6827	49.55677	49.16828	0.327878

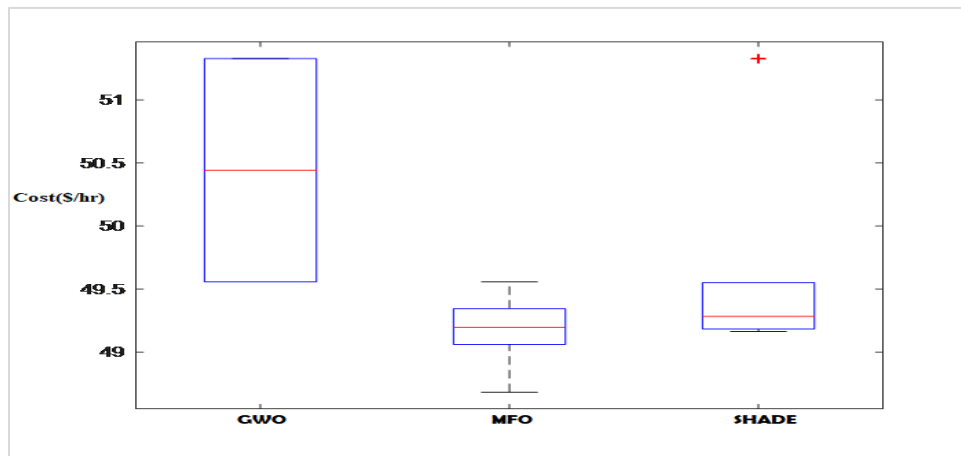


Figure 11 Boxplot being cost and emission minimization

4.2 An IEEE 57-bus system that has been changed

A modified version of the IEEE-57 bus could be used to test the system. Buses 6 and 12 feature a combination of solar PV and mild hydropower, while buses 9 and 12 each have a solar generator. This test system requires 13 variables: thermal power output on buses 2, 3, and 8; stochastic power generation (combined solar, micro hydro, and solar and wind generators) a voltage on each of these six power generation buses, and a single.

The lowest and maximum values for this system's control and state variables may be found in the MATPOWER package's case studies folder.

4.2.1 Case 1: lowering production costs

The overall outcomes obtained by combining MFO with the metaheuristic algorithms SHADE and GWO are displayed in Table 10. Based on the fact that

MFO and SHADE got different results from the IEEE 57 bus protocol, these two approaches have been chosen. MFO outperformed the other two strategies in relation to achieving the aim lowest price for the OPF issue. MFO has lowest generation cost at 30121.85 \$/h, while GWO has the highest generation cost at 30655.87 \$/h. SHADE obtained a comparable result to MFO, which was 30275.67 \$/h. The difference between MFO and SHADE values is 153.82 \$/h, suggesting considerable cost savings of $\$153.82 \text{ h} \times 8760 \text{ h} = \$1,338,703.2$ per year.

The potential profiles at the energy feeder generated by each technique shown in Figure 12; the bulk of them are similar in shape and limit 0.98 to 1.05 p.u.

Table 10 Statistic results for generation cost for different algorithms is based on this table

Innovation	Minimum(MW)	Maximum(MW)	Average value(MW)	Standard deviation(MW)
SHADE	30275.6722	32081.6722	32875.167	509.371673
MFO	30121.85	30750.98	31735.92	608.9789
GWO	30655.87	31730.35	31225.39	504.5374

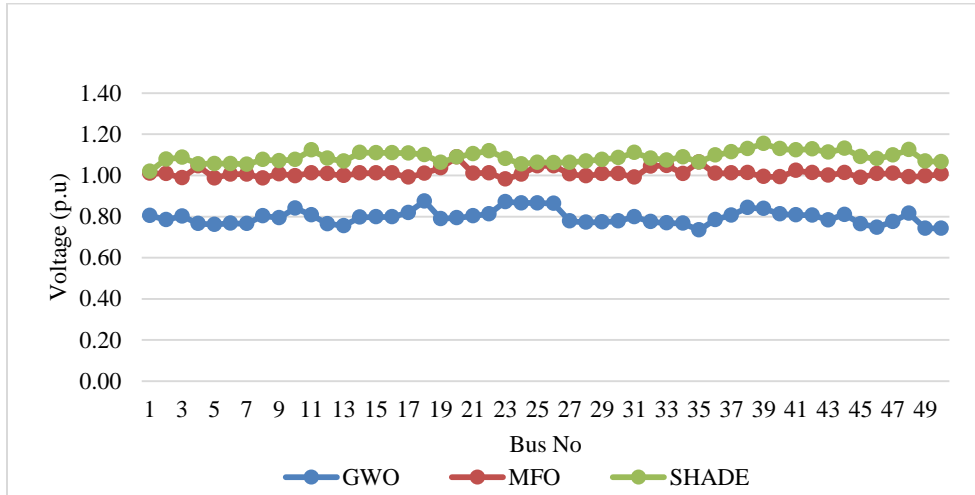


Figure 12 IEEE-57 bus voltage distribution for case 1

Analyzing the distribution results offered by all strategies for 30 trials, *Figure 13* depicts a boxplot for this case.

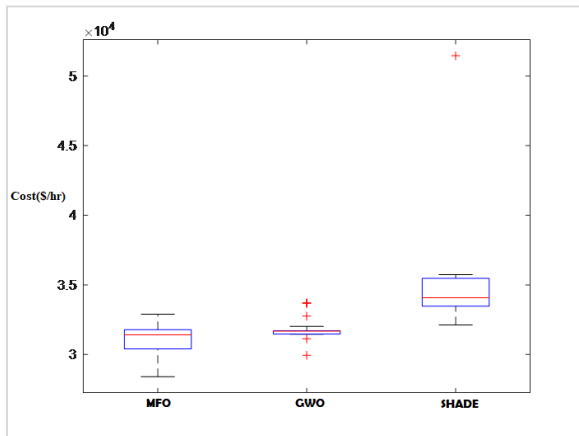


Figure 13 Box plot curve- case 1

When compared to other algorithms, this figure reveals that SHADE and GWO have more robust performance, but MFO has higher accuracy. Four values—6, 14, 22, and 26—reflecting 23 %, 50 %, 70 %, and 90 % of the earth's community, respectively, were used to examine the effects of changing the pl

must find a medium between exploiting the resource and discovering new things about it. Based on the findings of the simulation, the $Pl = 21$ parameters were shown to be the most advantageous outcome for each IEEE 30 and 57-feeder structure. This parameter produced the highest quality outcomes when contrasted with the other options.

4.2.2 Case 2: Less overall transmission loss

The target function in this case is to reduce transmission loss overall. The load flow program is conducted, and then the MATPOWER returns the overall loss. Note that MFO achieved the best loss reduction result according to *Table 11* with 19.70055 MW. The overall flexible main and secondary findings because of the redesigned IEEE 57-feeder protocol that is highlighted in *Tables 12* and *13*. The convergence curve is evident in *Figure 14*.

The IEEE 30-feeder and IEEE-57 feeder structure were optimized using MFO approaches. According to the data, the MFO is highly effective at resolving the OPF issue by lowering distribution dropping and production prices for preserving network safety (potential standard, lowest and highest load ranges).

Table 11 Minimization of total transmission loss

Innovation	Minimum(MW)	Maximum(MW)	Average value(MW)	Standard deviation(MW)
SHADE	21.76092	23.80031	0.16159	24.76878
MFO	19.70055	20.66049	0.370332	20.12781
GWO	20.24059	22.23845	0.783371	20.96234

Table 12 Optimal control variable findings for Cases 1-2

Item	Limit		Case 1		Case 2	
	Min	Max	GWO	MFO	GWO	MFO
Pg2	0.00	100.00	49.89	26.24	51.90	9.56
Pg5	0.00	140.00	75.00	75.00	136.69	140.00
Pg8	0.00	100.00	34.60	35.00	97.15	100.00
Pg11	0.00	550.00	57.44	60.00	315.76	315.96
Pg13	0.00	200.00	18.29	39.24	198.28	200.00
V _{g1}	0.00	210.00	1.06	1.06	210.00	210.00
V _{g2}	0.95	1.10	1.05	1.05	1.03	1.02
V _{g5}	0.95	1.10	1.04	1.04	1.07	1.10
V _{g8}	0.95	1.10	1.10	1.10	1.02	1.02
V _{g11}	0.95	1.10	1.10	1.10	1.04	1.02
V _{g12}	0.95	1.10	1.04	1.03	1.03	1.03
V _{g13}	0.95	1.10	1.03	1.02	0.98	1.10
V _{g14}	0.95	1.10	1.4	1.05	0.98	0.98
Cost(\$/h)			2.0108334562	1.73864886	31364.7846739117	29574.61785
Floss(MW)			2.106456965	2.07457453	20.05246417	19.68200787

Table 13 State variable results for Cases 1-2

State variables	Limit		Case1		Limit		Case 2	
	Min	Max	MFO	GWO	Min	Max	MFO	GWO
Pg1	50	200	50.86651 MW	50.53166 MW	0	450	376.01682 MW	377.28608 MW
Qg1(Mvar)	-20	150.0	-20.00000	-20.00000	-140	200	28.61165	76.82446
Qg2(Mvar)	-20	60.0	21.49194	18.25091	-17	50	50.00000	50.00000
Qg5(Mvar)	-30	35.0	19.80614	21.87291	-10	60	47.61349	-1.89348
Qg8(Mvar)	-15	40.0	40.00000	40.00000	-8	25	12.86673	25.00000
Qg11(Mvar)	-25	30.0	30.00000	29.40358	-140	200	52.52669	57.82163
Qg13(Mvar)	-20	25.0	18.29288	21.26882	-3	9	9.00000	9.00000

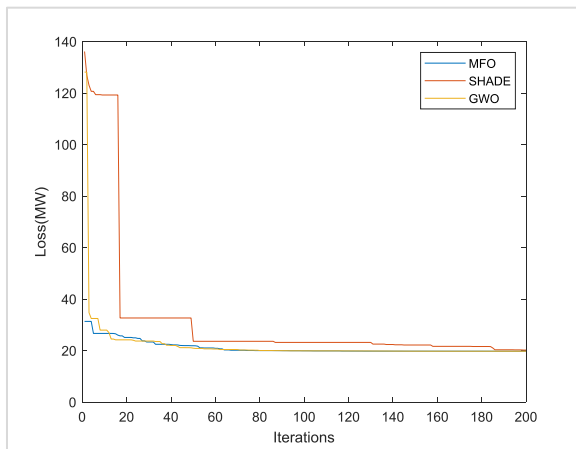


Figure 14 Convergence curve -case 2

4.2.3 Case 3: decrease in voltage deviation

Case 3 focuses on lowering voltage deviation because it has an impact on each bus's quality of voltage and is crucial to the power system network. *Table 14* displays the simulation results for this scenario.

MFO has been demonstrated to produce the lowest voltage variation yet giving superior findings expressed as max, mean, and std dev. The lowest voltage deviation reduction result, which comes from MFO, is 0.898822p.u. The load-specific voltage profiles buses produced by all techniques for this scenario are shown in *Figure 15*, the majority of which have a similar pattern and a p.u. between 0.98 and 1.05.

Table 14 Voltage deviation

Innovation	Minimum(p.u)	Maximum(p.u)	Average value(p.u)	Standard deviation(p.u)
SHADE	0.956523	1.05432	1.01982	0.065429
MFO	0.898822	1.035527	1.03101	0.077822
GWO	0.953718	1.082556	1.03813	0.057878

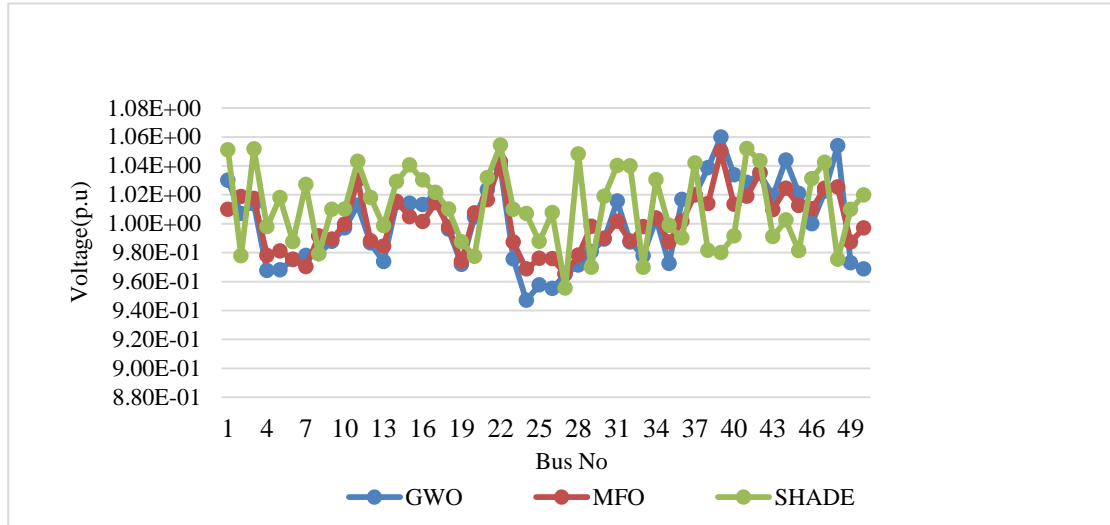


Figure 15 Voltage profile for case 3

4.2.4 Case 4: Emission reduction

The target function in this scenario is to reduce emissions. The statistical results for all approaches after 30 simulation trials are demonstrated in *Table 15*. The results of lowest, highest, mean, and SD

emission minimization achieved using MFO are highlighted. MFO outperforms others in terms of all statistical descriptors, as shown by the boxplot in *Figure 16*.

Table 15 Methods for the reduction of emissions

Innovation	Minimum(t/hr)	Maximum(t/hr)	Average value(t/hr)	Standard deviation(t/hr)
SHADE	1.761888	1.762467	1.762134	0.000245
MFO	1.013588	1.222048	1.163162	0.086073
GWO	1.197978	1.361709	1.280448	0.065786

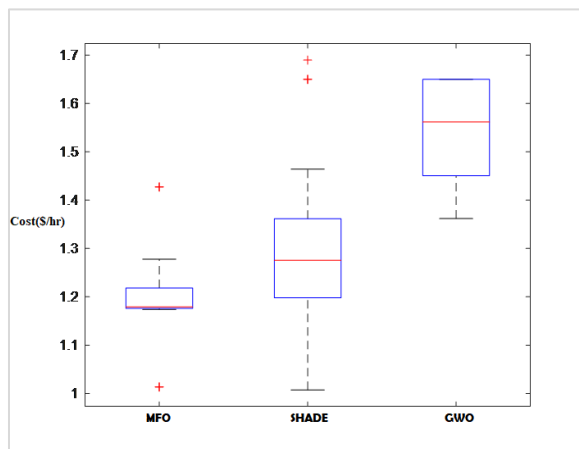


Figure 16 Boxplot for case 4

4.2.5 Case 5: Reducing generating costs and emissions

The main desire in this situation is a price reduction, that includes the emission impact. *Table 16* shows the detailed results. MFO outperformed GWO and SHADE at a cost of 248.4547 \$/hr vs 281.2938 \$/hr and 252.9079 \$/hr, respectively. It is worth noticing that MFO produced a little better result than GWO in this scenario. The difference in results between MFO and GWO is 32.8391 \$/h, which equates to $32.8391/h \times 8760 h = \$ 287670.516$ cost savings per year.

The boxplot for all strategies utilized to tackle this problem is shown in *Figure 17*.

Table 16 Reduction of production including emissions prices

Innovation	Minimum(MW)	Maximum(MW)	Average value(MW)	Standard deviation(MW)
SHADE	252.9079	134.9079096	134.9079096	2.59032E-12
MFO	248.4547	304.7858	284.1007	22.41016
GWO	281.2938	310.1459	12.64427	297.2727

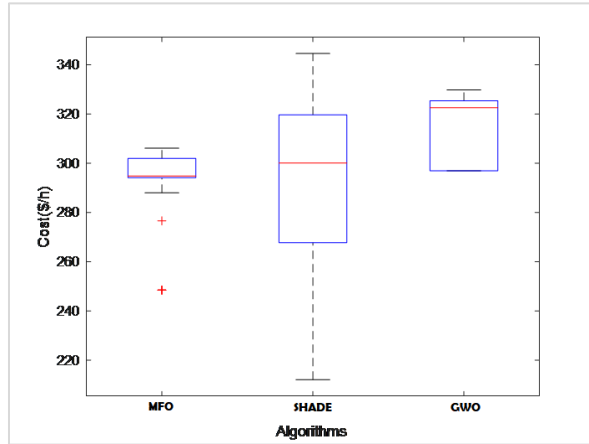


Figure 17 Boxplot for case 5

The SHADE and GWO algorithms do not coincide when a uniform began or a midway location is employed, however all methods coincide when the first point is an initial load move colloid. The initial step lengths of the LP iterate are too close to zero due to insufficient centrality, which prevents convergence. The MFO algorithm converged in each case. The MFO algorithm executes a similar amount of outer iterations for each of its three initializations (6 to 9 iterations).

5. Discussion

In order to address the OPF issue, this work suggests MFO, a brand-new evolutionary-based metaheuristic algorithm. We assessed the effectiveness of MFO in addressing OPF issues by applying it to five different OPF objective functions on two well-known test systems. Cost, transmission loss, emission costs, voltage stability, and generating costs, including emission costs, were all factors that we examined. Analyses of statistics and comparisons demonstrate that MFO routinely outperforms most algorithms and generates results that are very competitive. The variables gSG and gHG present in equation (4) and in (6) become more significant as the number of binding inequalities in the ideal solution increases, and the accuracy of the least-squares estimate declines. MFO power production costs being IEEE 30-feeder and IEEE 57-feeder structure are 888.7248 \$/h and 31121.85 \$/h, corresponding is 1.23% and 1.92% less expensive per hour than the least expensive values

discovered when comparing techniques. The annual price gaining’s for the IEEE 30-feeder and IEEE 57-feeder structures are estimated to be \$1,338,703.2 and \$28, 7670.516, respectively.

5.1 Limitation to the implementation of online OPF

Both study and closed-loop implementation methods are used for online OPF applications. The OPF results are offered to the express as suggestions in the study process. The design of an OPF’s interface with other online operations that are conducted at various periodicities is a significant challenge when the OPF is operating in closed-loop mode. Individual use, traditional ED, real-time sequence, security analysis, AGC, and others are a few of these features. Emphasis should be placed on creating consistency between these functions and static optimal solutions generated by the OPF to lessen the disparity between idealized and reality OPF situations. In situation 1 the best-scheduled value for two wind farms was found to be the rated value after setting punishment price factor (K_p) and reserve cost coefficient (K_R) to the lowest value of 0.01 (\$/kwh). It is not unreasonably expensive to acquire electricity from another source, regardless of how much breeze there is generated less of the expected total. The lowest total generation cost was achieved with an underestimation cost of 0 (USD/hr), overestimation cost of 69.95 (\$/hr), and final production price of 888.7248 (\$/hr), with wind farms contributing the most to the power system and thermal units contributing the least. Consistency needs the OPF to be properly integrated and interfaced with these functions.

The toughest demands on technology are made by online implementations. smooth nonlinear programming formulations of the classic formulations are much too hazy depictions of the real-world issues to result in good connected execution. Realistic operational and security consideration modeling has advanced significantly, but much more work is still required to build OPF-model-based systems that will either result in specialized tools or elements of separate power flow analysis software intricate operational processes. Most relevant key conditions—which must be

fulfilled for an online OPF package to be successfully implemented and used—were briefly discussed.

6. Conclusion and future work

The proposed MFO might offer an answer to the OPF problem. The investigation into utilizing multiple-objective metaheuristic design for multi-objective OPF issues will be covered in more detail shortly. Additionally, MFO obviously needs additional processing time to provide a better response. On the other hand, employing the parallel computing paradigm may reduce the computational cost, creating new chances and difficulties for MFOs to grow going forward. The following are major areas in which the study contributed:

Incorporate the MFO for an OPF solution for the modification of systems powered by stochastic wind, solar, and micro-hydro using the IEEE 30 and IEEE57 feeders.

- 1) An evaluation of the MFO vs earlier metaheuristic algorithms used in OPF solutions.
- 2) We believe our key contribution will be the incorporation of MFO into OPF alongside stochastic wind, solar, and micro-hydroelectric power generation.

To assess the MFO algorithm's performance in big systems, an actual 1211-feeder structure is employed. Due to the low voltage magnitudes on some buses, the constrained voltage limit ranges, and the absence of shunt correction in the optimization, this system is challenging to optimize.

Here are a few topics for further study:

- 1) The proposed MFO algorithms have rather static parameter settings. To increase the dynamism in the linked parameters, we advise combining yet another system of MFO techniques. Reduced transaction time is necessary for integration with other computer technologies, such as parallel computing.
- 2) To conduct an experiment to see if the MFO algorithm outperforms random search and to quantify how much better the MFO method outperforms random search.
- 3) To solve dynamic challenges, more literature is needed.
- 4) Real-world issues need to be solved by parameter adjustment. Sadly, the investigators make no attempt to investigate the MFO specifications.
- 5) More study on the theoretical side of MFO is required for it to be more stable.

- 6) To address more challenging large-scale multi-objective optimization issues, further study is necessary.

Acknowledgment

The University Malaysia Pahang (UMP) Doctoral Research Scheme (DRS) is funding this research for semester I, 2021/2022.

Conflicts of interest

The authors have no conflicts of interest to declare.

Author's contribution statement

Mohammad Khurshed Alam and Md. Shaoran Sayem did the study and drafted the article. **Mohd Herwan Sulaiman and Rahat Khan:** Examined the data and revised the manuscript for the journal. The final version had been authorized by all.

References

- [1] Risi BG, Riganti-fulginei F, Laudani A. Modern techniques for the optimal power flow problem: state of the art. *Energies*. 2022; 15(17):1-20.
- [2] Ramesh S, Vydeki D. Rice disease detection and classification using deep neural network algorithm. In *micro-electronics and telecommunication engineering: proceedings of 3rd ICMETE 2019* (pp. 555-66). Springer Singapore.
- [3] Happ HH. Optimal power dispatch. *IEEE Transactions on Power Apparatus and Systems*. 1974; 3:820-30.
- [4] Fioretto F, Mak TW, Van HP. Predicting AC optimal power flows: combining deep learning and Lagrangian dual methods. In *proceedings of the AAAI conference on artificial intelligence 2020* (pp. 630-7).
- [5] Fortenbacher P, Demiray T. Linear/quadratic programming-based optimal power flow using linear power flow and absolute loss approximations. *International Journal of Electrical Power & Energy Systems*. 2019; 107:680-9.
- [6] Montoya OD, Gil-gonzález W, Garces A. Sequential quadratic programming models for solving the OPF problem in DC grids. *Electric Power Systems Research*. 2019; 169:18-23.
- [7] Mohamed AA, Kamel S, Hassan MH, Mosaad MI, Aljohani M. Optimal power flow analysis based on hybrid gradient-based optimizer with moth-flame optimization algorithm considering optimal placement and sizing of FACTS/wind power. *Mathematics*. 2022; 10(3):1-31.
- [8] Obinwa CI, Nwabueze CA, Mbachu CB. Primal-dual interior-point technique for optimisation of 330kV power system on one variable. *European Journal of Engineering and Technology Research*. 2020; 5(2):165-70.
- [9] Krishnasamy V. Genetic algorithm for solving optimal power flow problem with UPFC. *International Journal of Software Engineering and Its Applications*. 2011; 5(1):39-50.

- [10] Singh A, Singh AD, Singh V. Optimal power flow solution of transmission line network of electric power system using genetic algorithm technique. *International Research Journal of Engineering and Technology*. 2018; 5(4):755-60.
- [11] Anwer A, Almosawi AH. A dynamic optimal power flow of a power system based on genetic algorithm. *Engineering and Technology Journal*. 2022; 40(2):290-300.
- [12] Duman S, Rivera S, Li J, Wu L. Optimal power flow of power systems with controllable wind-photovoltaic energy systems via differential evolutionary particle swarm optimization. *International Transactions on Electrical Energy Systems*. 2020; 30(4):1-28.
- [13] Widarsono K, Murdianto FD, Nur M, Mustofa A. Optimal power flow using particle swarm optimization for IEEE 30 bus. In *journal of physics: conference series 2020* (pp. 1-9). IOP Publishing.
- [14] Abido MA. Optimal power flow using particle swarm optimization. *International Journal of Electrical Power & Energy Systems*. 2002; 24(7):563-71.
- [15] Wang Z, Menke JH, Schäfer F, Braun M, Scheidler A. Approximating multi-purpose AC optimal power flow with reinforcement trained artificial neural network. *Energy and AI*. 2022; 7:1-13.
- [16] Moradi B, Kargar A, Abazari S. Transient stability constrained optimal power flow solution using ant colony optimization for continuous domains. *IET Generation, Transmission & Distribution*. 2022; 16(18):3734-47.
- [17] Al-bahran LT, Abdulrasool AQ. Multi objective functions of constraint optimal power flow based on modified ant colony system optimization technique. In *IOP conference series: materials science and engineering 2021*(pp. 1-18). IOP Publishing.
- [18] Suresh V, Janik P, Jasinski M. Metaheuristic approach to optimal power flow using mixed integer distributed ant colony optimization. *Archives of Electrical Engineering*. 2020; 69(2):335-48.
- [19] Dwivedi D, Balasubbareddy M. Optimal power flow using hybrid ant lion optimization algorithm. *Pramana Research Journal*. 2019; 9(2):368-80.
- [20] Addisu M, Salau AO, Takele H. Fuzzy logic based optimal placement of voltage regulators and capacitors for distribution systems efficiency improvement. *Heliyon*. 2021; 7(8):1-9.
- [21] Belboul Z, Toual B, Kouzou A, Mokrani L, Bensalem A, Kennel R, et al. Multiobjective optimization of a hybrid PV/wind/battery/diesel generator system integrated in microgrid: a case study in Djelfa, Algeria. *Energies*. 2022; 15(10):1-30.
- [22] Benzaouia M, Hajji B, Rabhi A, Mellit A, Benslimane A, Dubois AM. Energy management strategy for an optimum control of a standalone photovoltaic-batteries water pumping system for agriculture applications. In *proceedings of the 2nd international conference on electronic engineering and renewable energy systems: ICEERE, Saidia, Morocco 2021* (pp. 855-68). Springer Singapore.
- [23] Adetokun BB, Muriithi CM. Application and control of flexible alternating current transmission system devices for voltage stability enhancement of renewable-integrated power grid: a comprehensive review. *Heliyon*. 2021; 7(3):1-7.
- [24] Sadat SA, Sahraei-ardakani M. Customized sequential quadratic programming for solving large-scale ac optimal power flow. In *north American power symposium 2021* (pp. 1-6). IEEE.
- [25] Yalman Y, Çelik Ö, Adnan TA, Bayindir KÇ. Optimum power flow by using interior point optimization method. *Researcher*. 2022; 2(2):131-8.
- [26] Sun S, Li Y, Xu Z, Li M, Wang C. Research on AC/DC power flow optimization by using interior point method. In *IOP conference series: materials science and engineering 2019* (pp. 1-10). IOP Publishing.
- [27] Fang M, Xiang Y, Li J. Locational electricity-carbon price model: design and analysis. *Energy Reports*. 2022; 8:721-8.
- [28] Wang Z, Anderson CL. A progressive period optimal power flow for systems with high penetration of variable renewable energy sources. *Energies*. 2021; 14(10):1-17.
- [29] Hou Y, Gao H, Wang Z, Du C. Improved grey wolf optimization algorithm and application. *Sensors*. 2022; 22(10):1-19.
- [30] Basetti V, Rangarajan SS, Shiva CK, Pulluri H, Kumar R, Collins RE, et al. Economic emission load dispatch problem with valve-point loading using a novel quasi-oppositional-based political optimizer. *Electronics*. 2021; 10(21):1-21.
- [31] Li Q, Wang Z, Wei A. Research on optimal scheduling of wind-pv-hydro-storage power complementary system based on BAS algorithm. In *IOP conference series: materials science and engineering 2019* (pp. 1-9). IOP Publishing.
- [32] Bhende CN, Panda S, Mishra S, Narayanan A, Kaipia T, Partanen J. Optimal power flow management and control of grid connected photovoltaic-battery system. *International Journal of Emerging Electric Power Systems*. 2019; 20(5):1-16.
- [33] Omotoso HO, Al-shaalan AM, Farh HM, Al-shamma'a AA. Techno-economic evaluation of hybrid energy systems using artificial ecosystem-based optimization with demand side management. *Electronics*. 2022; 11(2):1-22.
- [34] Wais DS, Majeed WS. Performance of high voltage transmission line based on thyristor-control series compensator. *Journal of Engineering and Sustainable Development*. 2021; 25(5):26-38.
- [35] Ashour A, Mohamad TI, Sopian K, Ludin NA, Alzahrani K, Ibrahim A. Performance optimization of a photovoltaic-diesel hybrid power system for Yanbu, Saudi Arabia. *AIMS Energy*. 2021; 9(6):1260-73.
- [36] Biswas P, Suganthan P, Amaratunga G. Optimal power flow solutions using algorithm success history based adaptive differential evolution with linear population reduction. In *international conference on*

systems, man, and cybernetics 2018 (pp. 249-54). IEEE.

- [37] Sharma A, Sharma A, Averbukh M, Rajput S, Jatly V, Choudhury S, et al. Improved moth flame optimization algorithm based on opposition-based learning and Lévy flight distribution for parameter estimation of solar module. *Energy Reports*. 2022; 8:6576-92.
- [38] Ruta W, Saulo M, Odero NA. Emission constrained economic dispatch using moth flame optimization and bat hybrid algorithm. *International Journal of Engineering Research & Technology*. 2018; 11(5):827-44.
- [39] Alam MK, Sulaiman MH, Sayem MS, Imtiaz S, Khan R. Moth flame optimization for transmission loss minimization in optimal power flow using renewable energy. The 5th national conference for postgraduate research 2022 (pp. 1-6).
- [40] Sulaiman MH, Mustaffa Z, Mohamad AJ, Saari MM, Mohamed MR. Optimal power flow with stochastic solar power using barnacles mating optimizer. *International Transactions on Electrical Energy Systems*. 2021; 31(5):1-19.
- [41] Rahman SI, Hazari MR, Hani SU, Pathik BB, Mannan MA, Mahfuz A, et al. Primary frequency control of large-scale PV-connected multi-machine power system using battery energy storage system. *International Journal of Power Electronics and Drive Systems*. 2021; 12(3):1862-71.
- [42] Peter G, Stonier AA, Gupta P, Gavilanes D, Vergara MM, Lung SJ. Smart fault monitoring and normalizing of a power distribution system using IoT. *Energies*. 2022; 15(21):1-22.
- [43] Babu MT, Nei H, Kowser MA. Prospects and necessity of wind energy in Bangladesh for the forthcoming future. *Journal of The Institution of Engineers (India): Series C*. 2022; 103(4):913-29.
- [44] Rabbani MG, Sattary CT, Mamun MRA, Rahman MM, Khan MNH. Performance analysis of non-renewable energy in Bangladesh. *Indonesian Journal of Electrical Engineering and Computer Science*. 2017; 5(2):290-8.
- [45] Babayomi OO, Dahoro DA, Zhang Z. Affordable clean energy transition in developing countries: pathways and Technologies. *Iscience*. 2022; 25(5):1-6.
- [46] Sakthivel VP, Sathya PD. Single and multi-area multi-fuel economic dispatch using a fuzzified squirrel search algorithm. *Protection and Control of Modern Power Systems*. 2021; 6(1):1-13.
- [47] Mirjalili S. Moth-flame optimization algorithm: a novel nature-inspired heuristic paradigm. *Knowledge-Based Systems*. 2015; 89:228-49.



Mohammad Khurshed Alam, (L), BN(Retd) was born on 14 October 1968. He joined Bangladesh Navy on 14 July 1987. He was commissioned in the Electrical branch of Bangladesh Navy on 01 Jan 1990. He did his

graduation from the Bangladesh University of Engineering & Technology (BUET) in the Electrical & Electronics Engineering discipline in 1993. In 1998 he went to UK & Germany for Operation & Maintenance Training of PAXMAN Engine. He has done Navy Missile Maintenance Course from 2002 to 2003 in PRC. Moreover, he joined the UN Mission in Côte d'Ivoire as a contingent member from 2006 to 2007 and in D R Congo and CAR as a military observer from 2013 to 2014. He obtained a First Class in Masters of Electrical & Electronics Engineering from Khulna University of Engineering & Technology (KUET), Bangladesh in 2013. Retd Lt Cdr M. K. Alam served as the Weapons Electrical Officer on a seagoing frigate-BNS OSMAN, as well as the electrical officer, engineer officer, and missile officer on board other Bangladesh Navy ships. He is currently pursuing his doctorate at UMP in Malaysia while also holding a position as an Assistant Professor of FE at AIUB in Dhaka since Sep 2019.
Email: pes20002@stdmail.ump.edu.my



Mohd Herwan Sulaiman obtained his B. Eng. (Hons) in Electrical-Electronics, M. Eng (Electrical-Power) and PhD (Electrical Engineering) from Universiti Teknologi Malaysia (UTM) in 2002, 2007 and 2011 respectively. He is currently serves as an Associate Professor at Faculty of Electrical & Electronics Engineering, Universiti Malaysia Pahang (UMP). His research interests are power system optimization and swarm intelligence applications to power system studies. He is one of the main inventors of new nature inspired optimization algorithm namely Barnacles Mating Optimizer (BMO). He is also a Senior Member of IEEE. Love to write & ride. Now he is also a runner.
Email: herwan@ump.edu.my



Md. Shaoran Sayem received his B.Sc. Engg. and M.Sc. Engg. Degrees in Electrical and Electronic Engineering from American International University-Bangladesh (AIUB) in January 2020 and December 2021. After his B.Sc. degree, He served as an Intern in the Service Assurance Management department at Banglalink Digital Communication Ltd. Currently, he is working as a Network Engineer in the Data Analysis department at LM Ericsson Bangladesh Limited. He received several Academic Excellence Awards from AIUB for outstanding research and performance during the 2016-2021 academic year. His research interests are Renewable Energy Systems (especially Wind Power & Photovoltaic Power Systems), Power System Stability And Control, Microgrid and Hybrid Power Systems, HVDC System, Analysis and Control of Rotating Electrical Machines.
Email: shaoranmss@gmail.com



Rahat Khan received his B.Sc Engg from Minnesota State University, USA (MNSU) on December 2013 in Electrical engineering. Currently he is working as a Commercial planner for Banglalink Digital in Bangladesh. His research interests are Renewable Energy System, Power System Stability and Control, Micro Grid and Hybrid Power System.
Email: rahat.khan023@gmail.com

Appendix I

S. No.	Abbreviation	Description
1	AC	Alternating Current
2	AGC	Automatic Gain Control
3	AI	Artificial Intelligence
4	ANN	Artificial Neural Networks
5	CEED	Combined Economic and Emission Dispatch
6	CH	Constraint Handling
7	CI	Computational Intelligence
8	DE	Differential Evolution
9	DED	Dynamic Economic Dispatch
10	DFIG	Doubly Fed Induction Generator
11	DG	Distributed Generation Or Generator
12	EA	Evolutionary Algorithm
13	EC	Epsilon (ϵ) Constraint Handling Technique
14	ED	Economic Dispatch
15	EED	Economic Environmental Dispatch
16	EMS	Energy Management Systems
17	FACTS	Flexible Alternating Current Transmission System
18	GWO	Grey Wolf Optimization
19	HAPF	Hybrid Active Power Filter
20	IEEE	Institute of Electrical and Electronics

21	ISO	Independent System Operator
22	K_p	Penalty Cost Coefficient
23	K_R	Reserve Cost Coefficient
24	LSHADE	Linear Success History Based Adaptive Differential Evolution
25	LP	Linear Programming
26	MFO	Moth Flow Optimization
27	MOEA	Multi Objective Evolutionary Algorithm
28	MOEED	Multi Objective Economic Environmental Dispatch
29	MOOPF	Multi Objective Optimal Power Flow
30	MOP	Multi Objective Optimization Problem
31	OPF	Optimal Power Flow
32	ORPD	Optimal Reactive Power Dispatch
33	PSO	Particle Swarm Optimization
34	PDF	Probability Density Function
35	p.u.	Per Unit
36	PPA	Power Purchase Agreement
37	PV	Photovoltaic
38	RDN	Radial Distribution Network
39	SC	Shunt Capacitor
40	SF	Superiority of Feasible Solutions
41	SF-MFO	Superiority of Feasible Solutions Moth Flow Optimization
42	SHADE	Success History Based Adaptive Differential Evolution
43	SMODE	Summation Based Multi Objective Differential Evolution
44	UC	Unit Commitment
45	WT	Wind Turbine

Table A1 control variables for case 1-5 for IEEE-30 bus- results Different cases 1-5 detail results

Limit	Case 1			Case 2			Case 3			Case 4			Case 5		
	Mi	Max		MF	GW	SHA	MF	GW	SHA	MF	GW	SHA	MF	GW	SHA
Pg2	0.0	100.00	22.7	22.6	22.8	22.4	32.8	22.6	22.8	22.9	65	22.6	22.9	56	22.8
Pg5	0.0	140.00	15	15	15	15	25	15	20	45	15	25	55	25	15
Pg8	0.0	100.00	55	25	54	58	25	34	65	55	35	56	65	67	65
Pg1	0.0	550.00	33	36	54	57	4	55	52	55	15	90	220	35	450
Pg1	0.0	200.00	57	87	87	57	89	110	150	155	157	158	165	167	190
Vg	0.0	210.00	65	56	75	86	68	202	25	54	36	195	175	109	190
Vg	0.9	1.10	.99	.98	.96	.97	1	1.1	.98	.99	1	1.1	1.1	.98	1
Vg	0.9	1.10	1.1	.98	.97	1.1	1.1	1	.99	.98	.98	1	1.1	1	1.1
Vg	0.9	1.10	.98	.96	.98	.99	.99	1.1	1.1	1.1	.98	1	1.1	1	.98
Vg	0.9	1.10	.97	.99	.99	.98	.98	1	1	1	.98	.99	.98	.98	.99
Vg	0.9	1.10	.99	.98	1.1	.96	1.1	1.1	1.1	1.1	.99	.99	.98	.98	.99

Vg ₁₃	0.95	1.10	1	.96	1	.98	1	1	1.1	1	1.1	1	1.1	1.1	1	1.1	1
T _{6,9}	0.9	1.1	1	1.1	1	.9	1.1	.9	1.1	.9	1.1	.9	1.1	1	1	1.1	1
T _{6,10}	0.9	1.1	1.1	.9	1.0	1.1	.98	.9	1.1	1	1.1	.9	1	1.1	.9	1.1	1
T _{4,12}	0.9	1.1	1	1.1	1.1	.9	1.1	.9	1	1.1	1.1	.9	1	1.1	1.1	1.1	1.1
T _{28,27}	0.9	1.1	1.1	.9	.9	1	.9	1	1.1	.9	1	1.1	.9	.9	.9	1.1	1.1
Q _{c10}	0	5	5	1	0	5	0	5	0	5	0	5	0	5	0	5	0
Q _{c12}	0	5	0	5	1	5	5	1	0	5	0	5	0	1	5	1	0
Q _{c15}	0	5	0	5	5	4	5	2	5	3	5	4	0	1	4	3	0
Q _{c17}	0	5	0	3	3	5	5	3	3	5	3	3	3	1	5	3	3
Q _{c20}	0	5	0	4	3	5	3	5	5	3	5	5	5	5	4	5	5
Q _{c21}	0	5	0	5	0	5	0	5	5	0	5	0	5	0	5	0	5
Q _{c23}	0	5	5	4	3	4	2	4	5	2	4	3	4	3	4	5	3
Q _{c24}	0	5	5	4	4	3	5	4	5	5	5	4	5	4	2	3	5
Q _{c29}	0	5	5	3	2	3	4	5	4	5	2	5	4	2	5	3	2
Fuel Cost(\$/h)	Valve	888.7	889.9	891.2	898.7	899.9	896.2	887.7	888.9	899.2	898.7	888.9	898.2	896.7	885.9	897.2	
Q _{gen} (\$/h)		19.0	21.2	20.3	18.0	22.2	21.3	23.0	25.2	26.3	24.0	25.2	24.3	20.0	26.2	24.3	
W _{gen} cost(\$/h)		247.7	245.3	254.2	256.7	275.3	257.2	277.7	285.3	274.2	247.7	285.3	264.2	277.7	265.3	259.2	
P _{loss} (MW)		7	7.9	7	7	7.7	7	7	7.6	7	7	7.3	7	7	7.5	7	
G _{best} valur(\$/h)		782.6	783	785	786.6	787	788	786.6	787	775	772.6	793	795	772.6	783	785	
F _{Emission} (ton/h)		1.2	1.3	1.3	1.6	1.6	1.5	1.7	1.8	1.8	1.5	1.3	1.7	1.6	1.8	1.7	
Computation time(s)		81.5	78.7	77.3	85.5	88.7	87.3	86.5	98.7	78.3	86.5	88.7	87.3	86.5	74.7	78.3	

Table A2 Control variables for case 1-5 for IEEE-57 bus- results

Limit	Case 1					Case 2			Case 3			Case 4			Case 5		
Ite m	M in	Ma x	MF O	GW O	SHA DE	MF O	GW O	SHA DE	MF O	GW O	SHA DE	MF O	GW O	SHA DE	MF O	GW O	SHA DE
Pg ₂	0.00	100.00	22.7	22.6	22.8	22.4	56.8	52.6	82.8	72.9	65	92.6	82.9	56	22.8	82.9	22.8
Pg ₅	0.00	140.00	15	15	15	15	25	15	20	65	15	65	55	75	65	59	25
Pg ₈	0.00	100.00	55	25	54	58	25	34	65	55	35	56	65	67	65	55	25
Pg ₁₁	0.00	550.00	37	36	54	57	4	55	52	55	15	90	220	35	450	53	59
Pg ₁₃	0.00	200.00	57	43	87	57	89	110	150	155	157	158	165	167	190	185	97
Vg ₁	0.00	210.00	65	56	75	86	68	202	25	54	36	195	175	109	190	187	173
Vg ₂	0.95	1.10	.99	.98	.96	.97	1	1.1	.98	.99	1	1.1	1.1	.98	1	1.1	.99
Vg ₅	0.95	1.10	1.1	.98	.97	1.1	1.1	1	.99	.98	.98	1	1.1	1	1.1	1	1.1
Vg ₈	0.95	1.10	.98	.96	.98	.99	.99	1.1	1.1	1.1	.98	1	1.1	1	.98	1	.96
Vg ₁₁	0.95	1.10	.97	.99	.99	.98	.98	1	1	1	.98	.99	.98	.98	.99	1.1	.98
Vg ₁₂	0.95	1.10	.99	.98	1.1	.96	1.1	1.1	1.1	1.1	.99	.99	.98	.98	.99	1.1	1.1
Vg ₁₃	0.95	1.10	1	.96	1	.98	1	1	1.1	1	1.1	1	1.1	1.1	1	1.1	1

$T_{6,9}$	0.9	1.1	1	1.1	1	.9	1.1	.9	1.1	.9	1.1	.9	1.1	1	1	1.1	1
$T_{6,10}$	0.9	1.1	1.1	.9	1.0	1.1	.98	.9	1.1	1	1.1	.9	1	1.1	.9	1.1	1
$T_{4,12}$	0.9	1.1	1	1.1	1.1	.9	1.1	.9	1	1.1	1.1	.9	1	1.1	1.1	1.1	1.1
$T_{28,27}$	0.9	1.1	1.1	.9	.9	1	.9	1	1.1	.9	1	1.1	.9	.9	.9	1.1	1.1
Q_{c10}	0	5	5	1	0	5	0	5	0	5	0	5	0	5	0	5	0
Q_{c12}	0	5	0	5	1	5	5	1	0	5	0	5	0	1	5	1	0
Q_{c15}	0	5	0	5	5	4	5	2	5	3	5	4	0	1	4	3	0
Q_{c17}	0	5	0	3	3	5	5	3	3	5	3	3	3	1	5	3	3
Q_{c20}	0	5	0	4	3	5	3	5	5	3	5	5	5	5	4	5	5
Q_{c21}	0	5	0	5	0	5	0	5	5	0	5	0	5	0	5	0	5
Q_{c23}	0	5	5	4	3	4	2	4	5	2	4	3	4	3	4	5	3
Q_{c24}	0	5	5	4	4	3	5	4	5	5	5	4	5	4	2	3	5
Q_{c29}	0	5	5	3	2	3	4	5	4	5	2	5	4	2	5	3	2
Fuel Cost(\$/h)	Valve	3000	3010	3020	3020	3004	3050	3005	3020	3000	3040	3050	3010	3060	3060	3080	
Q_{gen} (\$/h)		119.	121.	120.	118.	212.	211.	223.	245.	266.	244.	235.	234.	240.	262.	244.	
W_{gen} cost(\$/h)		0	2	3	0	2	3	0	2	3	0	2	3	0	2	3	
P_{loss} (MW)		247.	245.	254.	256.	275.	257.	277.	285.	274.	247.	285.	264.	277.	265.	259.	
		7	3	2	7	3	2	7	3	2	7	3	2	7	3	2	
G_{best} valur(\$/h)		21	19	22	23	24	22	23	25	21	26	27	22	7	21	22	
$F_{Emission}$ (ton/h)		1782	1783	1785	1786	1787	1788	1786	1787	1775	1772	1793	1795	1772	1783	785	
		.6			.6			.6			.6			.6			
Computation time(s)		1.7	1.4	1.5	1.8	1.7	1.85	1.6	1.8	1.9	1.7	1.8	1.8	1.9	1.8	1.7	
		181.	178.	177.	185.	188.	187.	186.	198.	178.	186.	188.	187.	186.	174.	78.3	
		5	7	3	5	7	3	5	7	3	5	7	3	5	7		

Table A3 The ideal way to handle OPF problems

Function objective to be optimized	Suitable methods	Reason to use that method
Economic dispatch	EMS	Rapid method
ED with irregular cost functions	LP	Non-linear difficulty
Reactive power enhancement	AI,SF	Accurate procedures
The optimal placement of OPF devices	EMS,SF	Multipurpose nonlinear problem
OPF security restrictions	SF,LP	Consistent convergence
Congestion Management	SF	Multi objective nonlinear problem
Social fortune	SF,AI	Multidimensional nonlinear issue